Title
Turning a surface superrepellent even to completely wetting liquids

Journal
Science, 346(6213)

ISSN
0036-8075

Authors
Liu, Tingyi Leo
Kim, Chang-Jin CJ

Publication Date
2014-11-28

DOI
10.1126/science.1254787

Manuscript for: T. Liu and C.-J. Kim, "Turning a surface superrepellent even to completely wetting liquids," *Science*, vol. 346, no. 6213, pp. 1096–1100, Nov. 2014.

Turning a surface super-repellent even to completely wetting liquids*

Authors: Tingyi "Leo" Liu[1] and Chang-Jin "CJ" Kim[1,2]†

Affiliations:

[1]Mechanical and Aerospace Engineering Department, University of California, Los Angeles (UCLA), Los Angeles, CA 90095, USA

[2]Bioengineering Department, University of California, Los Angeles (UCLA), Los Angeles, CA 90095, USA

† Correspondence to: C.-J. Kim (cjkim@ucla.edu)

Abstract:

Superhydrophobic and superoleophobic surfaces have so far been made by roughening a hydrophobic material. However, no surfaces were able to repel extremely low-energy liquids, such as fluorinated solvents, which completely wet even the most hydrophobic material. We show how roughness alone, if made of a specific doubly re-entrant structure that enables very low liquid-solid contact fraction, can render the surface of any material super-repellent. We start from a completely wettable material (silica) and micro/nano-structure it to be truly superomniphobic, bouncing off even perfluorohexane. Same superomniphobicity is further confirmed with identical surfaces of a metal and a polymer. Free of any hydrophobic coating, the superomniphobic silica surface also withstands over 1000°C and resists biofouling.

One Sentence Summary:

Super-repellency is obtained solely from surface roughness regardless of the material's intrinsic wettability and demonstrated for all available liquids.

Main Text:

Understanding the extraordinary liquid repellency of natural surfaces (*1*, *2*) has affected a wide range of scientific and technological areas, from coatings (*3*), heat transfer (*4*), drag reduction (*5*), to biological applications (*6*). While the wetting-resistant surfaces developed since the 1960s (*7–10*) utilized only surface roughness to trap gas with no interest in the apparent contact angles, superhydrophobic surfaces since the late 1990s (*1*, *11*, *12*) combined the roughness with a hydrophobic material to super-repel water, i.e., display a very large apparent contact angle ($\theta^* > 150°$) and a very small roll-off angle ($\theta_{rolloff} < 10°$). For low energy liquids such as oils or organic solvents, a roughness with overhanging topology was necessary to make the hydrophobic material superoleophobic (*13*, *14*) or so-called omniphobic (*15*) or superomniphobic (*16*, *17*). Despite the use of prefix omni- (*6*, *15–18*), however, no natural or man-made surface has been reported to repel liquids of extremely low surface tension/energy (i.e., $\gamma < 15$ mJ/m^2), such as fluorinated solvents, which completely wet existing materials (*10*, *19–21*). Departing from the prevailing approach of roughening a hydrophobic material, we first propose the material's inherent wettability, depicted by the intrinsic contact angle θ_Y, is irrelevant when dealing with a completely wetting liquid ($\theta_Y = 0°$). Focusing instead solely on the roughness details, we develop a surface that super-repels all available liquids including fluorinated solvents, e.g., perfluorohexane (C_6F_{14}, viz. 3M™ Fluorinert™ FC-72) whose surface energy ($\gamma = 10$ mJ/m^2) is the lowest known and has never been observed to bead up, let alone roll off, on any surface.

To avoid the confusion with the petal effect (*22*), where a droplet with large contact angles sticks to the surface, it helps to first clarify that repelling means droplets not only bead up but also roll off on the surface. To repel (i.e., $\theta^* > 90°$ with a small $\theta_{rolloff}$) or super-repel ($\theta^* > 150°$ with $\theta_{rolloff} < 10°$) a wetting liquid ($\theta_Y < 90°$) on a structured surface, two conditions must be met: (1) a successful liquid suspension on the roughness and (2) a low liquid-solid contact. The microstructures should first be able to suspend the liquid, supporting a composite interface proposed by Cassie and Baxter (*23*). Once suspended, decreasing the liquid-solid contact would increase θ^* and reduce $\theta_{rolloff}$, hence increasing the repellency. The rare cases of a highly wetting ($\theta_Y < 10°$) liquid beading (i.e., successful suspension and $\theta^* > 90°$) on a structured surface, e.g., water on SiO_2 (*13*, *24*) and hexane on nickel (*16*), reported the liquid sticking on the surface rather than rolling off; they are not considered liquid repelling despite beading.

Liquid suspension by surface structures, or resisting liquid wetting by surface topologies with characteristic length smaller than the liquid's capillary length, has been proposed in the 1960s considering θ_Y as a critical parameter (*8*, *10*). For $\theta_Y > 90°$, such as water or aqueous solutions on a hydrophobic material, a simple microstructure (Fig. 1A) would suspend the liquid to a Cassie state (*1*, *2*, *8*, *10–12*) (figs. S1 and S2). For $\theta_Y < 90°$, such as oils and organic solvents on a hydrophobic material or water on a slightly hydrophilic material, a re-entrant microstructure (Fig. 1B) is required to suspend the liquid and resist it from wetting into the cavity (*3*, *8*, *10*, *13–18*, *25*). From simple force balance, the re-entrant topology of Fig. 1B would suspend a liquid even with $\theta_Y \sim 0°$ in the absence of any positive liquid pressure. However, there is always a pressure (e.g., hydrostatic, Laplace, environmental perturbation) in reality, and once pushed into the cavity the liquid spreads spontaneously. So far, the most successful suspension was for liquids with surface energy as small as $\gamma \sim 15$ mJ/m^2, i.e., pentane (*15*, *16*) and isopentane (*16*), leaving many fluorinated solvents unaccounted for.

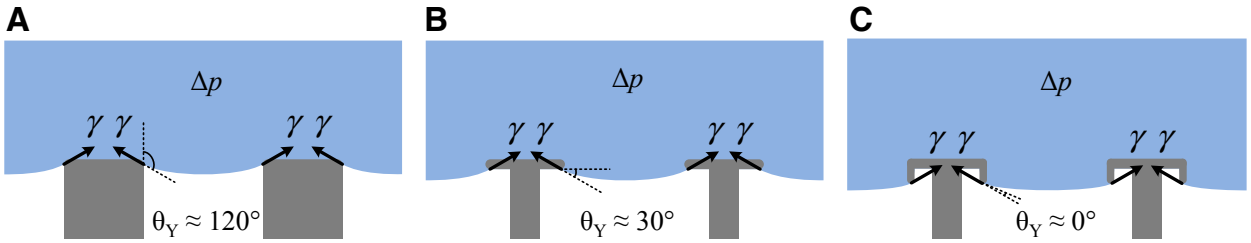

Fig. 1. Liquid suspension on surface structures of three different topologies. (**A**) Simple structures require $\theta_Y > 90°$ to suspend water. (**B**) Re-entrant structures allow $\theta_Y < 90°$ to suspend oil or solvents as well. They would fail if $\theta_Y \sim 0°$, as surface tension acts parallel to the horizontal overhangs with little vertical component to suspend the liquid. (**C**) Doubly re-entrant structures allow $\theta_Y \sim 0°$ to suspend any liquid, as surface tension acts on the vertical overhangs with a significant vertical component. If the liquid-solid contact fraction is small enough, the surfaces would also repel the liquids, as this paper aims.

In addition to the re-entrant microstructure, it has long been hypothesized that surface structures of a doubly re-entrant topology (Fig. 1C) might provide a stronger resistance against wetting and retain suspension even if $\theta_Y \sim 0°$ (*8–10*, *15*, *26*). The mechanism of suspending such a perfectly wetting liquid on a doubly re-entrant microstructure is reasoned as follows, using Fig. 1C. Upon contacting the surface, the liquid would wet the top surface and continue down along the sidewall of the vertical overhangs. The liquid would stop advancing at the bottom tip of the vertical overhangs, where the surface tension can start to point upwards. While this concept of suspending even highly wetting liquids on a doubly re-entrant topology has been known (*8–10*, *15*, *26*) and confirmed with water (*24*), for the resulting surface to not just suspend but repel the liquid the liquid-solid contact fraction should be sufficiently low. A highly wetting ($\theta_Y < 10°$) liquid suspended on the microstructures would still spread (i.e., $\theta^* < 90°$) on the composite surface unless the liquid rests mostly on air. To understand how far we are from being able to repel the highly wetting liquids, let us assess the contribution of air to the repellency.

The apparent contact angle θ^* for a suspended droplet (i.e., in Cassie state) is described by the Cassie-Baxter model (*23*) as

$$\cos\theta^* = f_s \cos\theta_Y - f_g \tag{1}$$

where f_s is the liquid-solid contact fraction, or solid fraction for short, i.e., the proportion of liquid-solid contact area (including the wetted regions inside the roughness) to the projected area of the entire composite interface, and f_g is the gas fraction similarly defined for liquid-vapor interface, and $f_s + f_g \geq 1$ (*27*). If the liquid-solid and liquid-vapor interfaces are perfectly flat (i.e., neglecting any solid roughness and meniscus curvature), i.e., the ideal Cassie state with $f_s + f_g = 1$, Eq. 1 simplifies to

$$\cos\theta^* = f_s (1 + \cos\theta_Y) - 1 \tag{2}$$

Although valid only for the ideal Cassie state, Eq. 2 allows us to qualitatively explore the relation between θ^*, f_s, and θ_Y. In addition to the widely appreciated consequence that θ^* can be greatly increased as f_s decreases, we examine the role of the intrinsic contact angle θ_Y by plotting Eq. 2

with θ_Y as a parameter in Fig. 2. It can be seen that the difference between the θ^* values of a large θ_Y and a small θ_Y decreases as f_s decreases. In other words, by minimizing f_s the contribution of the material's inherent non-wettability (described by the magnitude of θ_Y) on the liquid repellency (described by the magnitude of θ^*) diminishes. This diminishing trend suggests that a structured surface may repel extremely wetting liquids if f_s is very small. For example, even a completely wetting liquid (θ_Y = 0°) may be super-repelled (θ^* > 150°) if f_s < 6%. However, it should not be forgotten that this argument is valid only for the Cassie (i.e., suspended) state, which is exceedingly difficult to achieve if f_s becomes very small. Even for the re-entrant topology of Fig. 1B, the suspension force becomes too small before f_s becomes small enough to repel liquids with very small θ_Y. This difficulty explains why super-repellency has been shown for liquids with surface tensions above ~20 mN/m (*13*) but not for those with 15-20 mN/m, i.e., pentane (*15*, *16*) and isopentane (*16*), which have been suspended but not repelled.

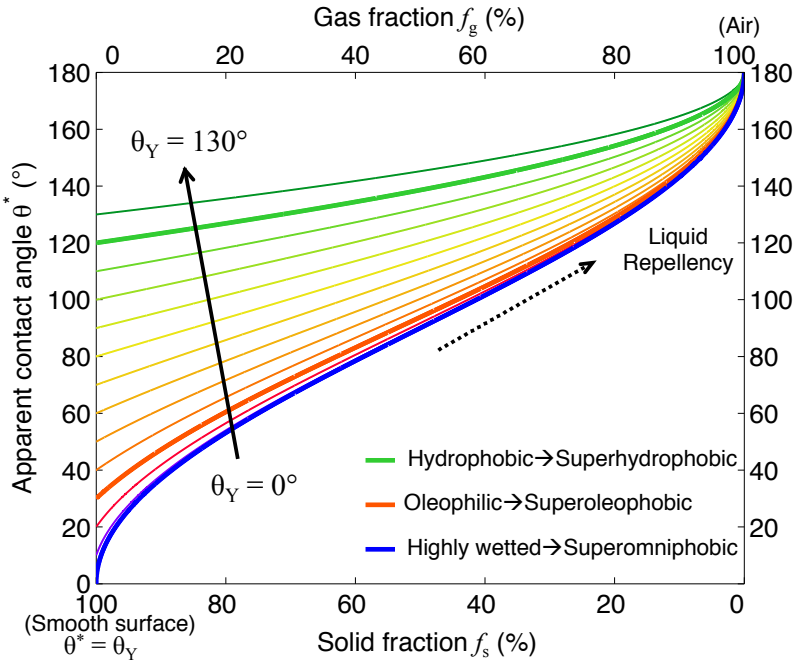

Fig. 2. Relationship between apparent contact angle θ^* and solid fraction f_s for ideal Cassie state droplets with intrinsic contact angle θ_Y as a parameter. As f_s decreases, the band of lines narrows, indicating that the influence of θ_Y on θ^* diminishes. If f_s is below 6%, θ^* is above 150° even if θ_Y ~0°. The greenish, reddish and bluish lines represent the inherent wettability: non-wetting (e.g., water on hydrophobic surface), moderately wetting (e.g., solvent on hydrophobic surface), and highly wetting (e.g., fluorinated solvents on any surface or most liquids on clean SiO_2), respectively. The three bold lines correspond to the three cases shown in Fig. 1.

From Figs. 1 and 2, one can now reason that a structured surface may repel any liquid if the microstructures are doubly re-entrant and also of a low enough solid fraction. However, common doubly re-entrant shapes in the literature (*8*, *10*, *15*, *18*, *26*) produce only a weak suspension and a moderate solid fraction insufficient to repel highly wetting liquids. To suspend extremely wetting liquids on a surface with a minimal solid fraction, an entire surface should be uniformly covered with doubly re-entrant structures having vertical overhangs as thin, vertical, and short as possible. Illustrated in Fig. 1C, such an ideal doubly re-entrant structure minimizes the break-in force by the liquid pressure that wets the cavity and maximizes the surface tension force that suspends the liquid against wetting (Eq. S1) (*9*). Importantly, the thin and vertical geometry of the overhangs minimizes their projected area added to the solid fraction, and the shortness of the overhang keeps the increase of the solid fraction by the vertical surfaces at bay. Some superhydrophobic or superoleophobic surfaces in the literature attempted to incorporate doubly re-entrant structures on them but with little success. For example, only a few doubly re-entrant structures were formed among predominantly simple or re-entrant structures prone to wetting (*3*, *14*, *25*), and structures barely satisfying the doubly re-entrant shape were replicated from springtail skin with only a moderate solid fraction (*18*).

To fulfill all the requirements reasoned above and quantified from Fig. 2, we designed a surface illustrated in Fig. 3A: an array of doubly re-entrant structures consisting of microscale posts with nanoscale vertical overhangs. Posts were chosen over ridges or holes to minimize f_s more easily. Also, the post array allows the air underneath the droplet to remain connected to the atmosphere so that the liquid is suspended only by surface tension and not assisted by the pressure of the trapped air. We chose to form the surface structures from silicon dioxide (SiO_2) for the following two reasons. First, clean SiO_2 is highly wetted (i.e., $\theta_Y < 10°$) by most liquids (except liquid metals like mercury) including water (*1*, *20*). Since roughening of a SiO_2 surface is supposed to amplify the liquid affinity to complete wetting (*1*), structuring a SiO_2 surface to repel liquids should provide a stark contrast to the existing approach. Second, silicon (Si) micromachining provides sophisticated equipment and techniques to process SiO_2. With precisely controlled thermal oxidation of a shallow-etched silicon surface followed by three sequential etching steps on SiO_2 and Si (fig. S3E)(*28*), we successfully fabricated a SiO_2 surface (1.7 cm × 1.7 cm) with close-to-ideal doubly re-entrant structures (Fig. 3B-E). The inclined angle of the vertical overhang is measured to be ~85±1° (Fig. 3E), providing a maximum suspension force that is 99.6% of the perfectly vertical overhang shown in Fig. 1C. In spite of the overall resemblance between the micro-posts in Fig. 3B and those of superoleophobic surfaces (*13*, *15–17*), it is the close-to-ideal nanoscale vertical overhangs in Fig. 3C-E that lead to an unprecedented liquid-repellency.

To evaluate the liquid repellency, we chose fourteen different liquids (Table S1)(*29*) including water, ionic liquid, acid, oils, and numerous polar or non-polar organic or fluorinated solvents with surface tensions ranging from 72.8 mN/m (i.e., water) to the lowest known 10 mN/m (i.e., FC-72). A smooth SiO_2 surface was highly wetted ($\theta^* = \theta_Y < 10°$) by all the liquids, as expected (Table S2). In contrast, our structured SiO_2 surface successfully suspended and repelled all of the tested liquids, beading them into Cassie state droplets (water, methanol, and FC-72 shown in fig. S4A and Movie S1) and letting them roll around (fig. S4B and Movies S2 and S3), i.e., behaving superomniphobic in air.

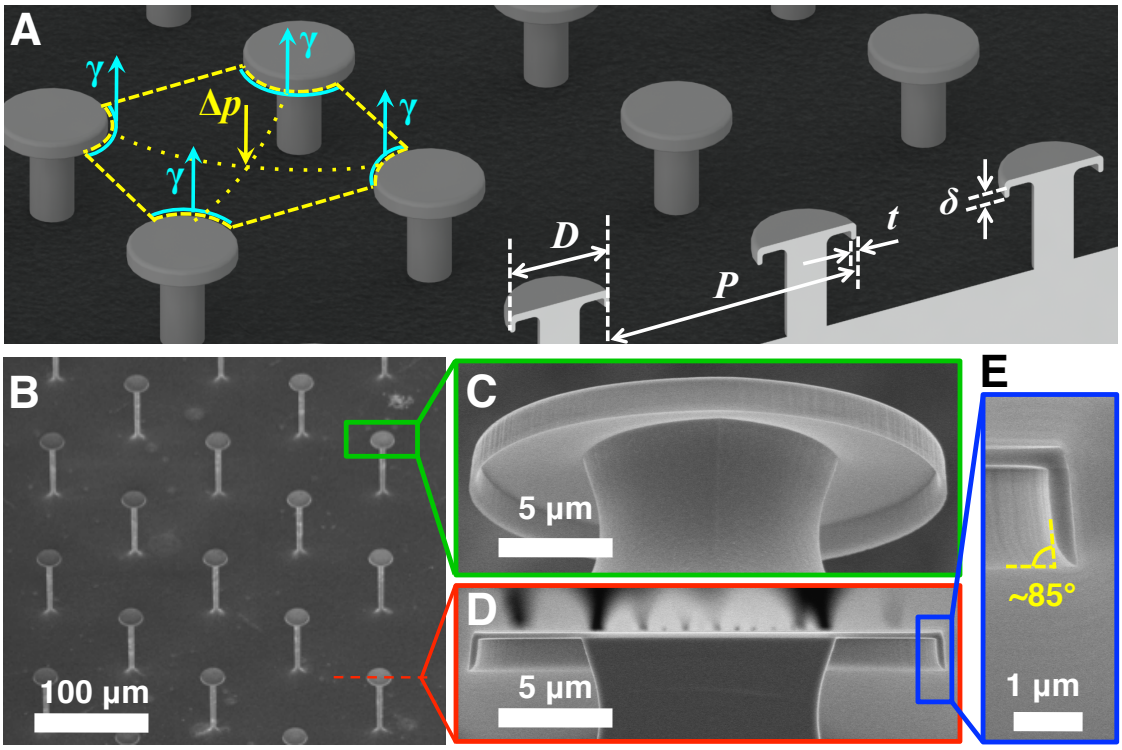

Fig. 3. Design and fabricated results of the SiO_2 surface. (**A**) Designed surface of micro-posts with doubly re-entrant nano-overhangs. As key geometric parameters, D is the post top diameter, P is the center-to-center distance (i.e., pitch) between adjacent posts, and δ and t are the length and thickness of the vertical overhang. To make f_s small enough ($f_s < 6\%$), δ and t should be shrunk to extreme values. (**B** to **E**) SEM micrographs of the fabricated surface: (**B**) top angled view of the square-array of circular posts with $D \sim 20$ μm, $P = 100$ μm, $\delta \sim 1.5$ μm, and $t \sim 300$ nm, resulting in $f_s \sim 5\%$; (**C**) bottom angled view of one post; (**D**) cross-sectional view of one post, and (**E**) magnified cross-sectional view of the vertical overhang. Note the similarity with the ideal topology of Fig. 1C.

To quantify the repellency of our surface, we measured the advancing and receding contact angles (Fig. 4A) and roll-off angles (fig. S4C) of all fourteen liquids. Fig. 4A also includes the other two liquid-repellent surfaces analyzed in Fig. 1 for comparisons: a superhydrophobic surface consisting of cylindrical posts (Fig. 1A and fig. S3B) and a superoleophobic surface consisting of posts with re-entrant overhangs (Fig. 1B and fig. S3D), both of which were coated with a hydrophobic layer of C_4F_8. Each data point is an average of over 100 measurements. The error bars are omitted in Fig. 4A for clarity and are instead shown in fig. S6. As expected, while the superhydrophobic surface with vertical posts could not suspend liquids with surface tension below ~40 mN/m, the superoleophobic surface with re-entrant posts repelled liquids with lower surface tension (20-40 mN/m). However, liquids with even lower surface tension (< 20 mN/m) could not be suspended as they wicked between the re-entrant posts. In contrast, on the surface with doubly re-entrant posts, all fourteen liquids formed large contact angles even without any hydrophobic coating.

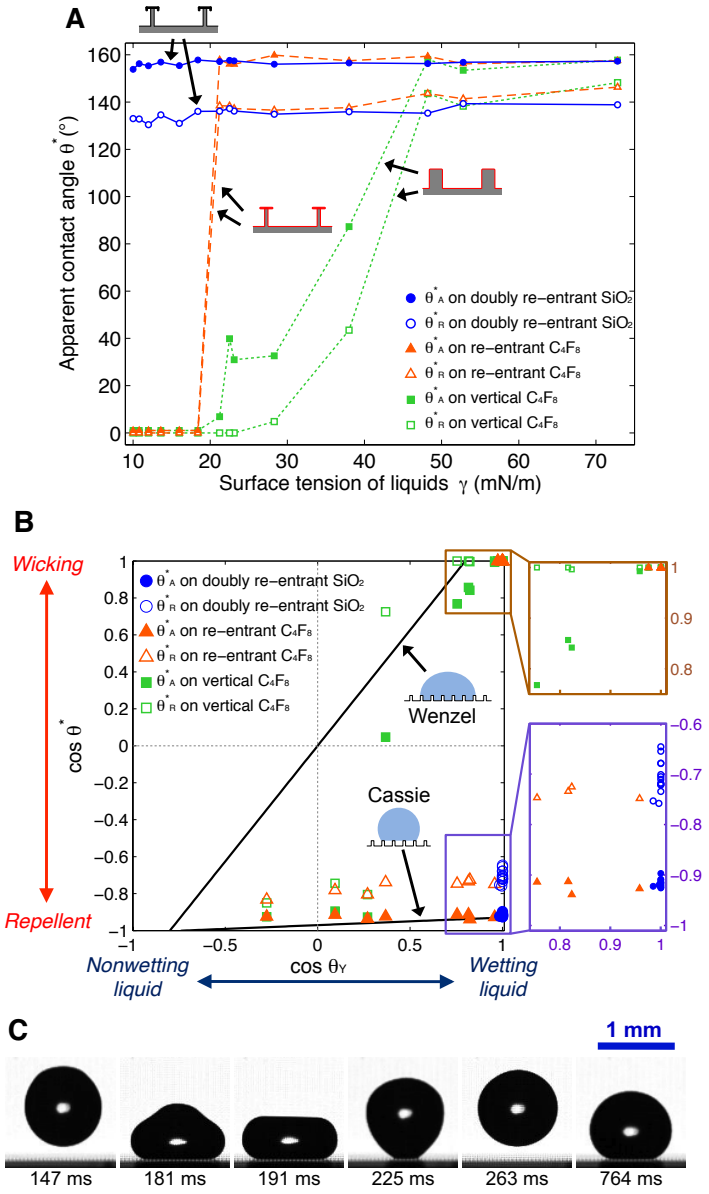

Fig. 4. Omniphobicity of the structured SiO_2 surface. (**A**) Apparent advancing and receding contact angles of the fourteen liquids measured on three liquid-repellent surfaces – our omniphobic surface and two control surfaces of the same nominal solid fraction (f_s ~5%). Data on the omniphobic surface are depicted in blue circles (solid and hollow). Data on the control surface with re-entrant and vertical topologies are depicted in orange triangles and green squares, respectively. (**B**) Relations of contact angles on smooth surface ($\cos\theta_Y$) and on a structured surface ($\cos\theta^*$). The theoretical relations from Wenzel and Cassie-Baxter models are plotted in solid black lines. Data near (1,-1) and (1,1) are shown in the zoomed-in boxes, revealing the difference between our structured SiO_2 surface with the control surfaces, especially when liquids highly wet the material. (**C**) Robust repellency of the structured SiO_2 surface demonstrated by bouncing FC-72 off the omniphobic SiO_2 surface with doubly re-entrant posts of D ~ 10 μm, P = 50 μm, δ ~ 920 nm, t ~ 270 nm, and f_s ~5% under Weber number We ~0.42.

The extent to which wettability is modulated by surface roughness is shown in Fig. 4B where the apparent wettability (i.e., cos θ^*) is plotted as a function of the inherent wettability (i.e., cos θ_Y). Data from our doubly re-entrant posts surface (i.e., blue circles) were populated at the lower right corner in the fourth quadrant near point (1,-1), exhibiting the exceptional ability to render a highly wettable material super-repellent. In contrast, while the two control surfaces permit a Cassie state with non-wettable or partially wettable material, they got soaked when the material was highly wetted by the liquids of very low surface tension (i.e., hexane and six fluorinated solvents), displaying $\theta^* \sim 0°$ with data populated near point (1,1). These results are consistent with the theory schematically summarized in fig. S2.

In addition to repelling all fourteen liquids (Movie S2), our superomniphobic surfaces are also expected to sustain static (fig. S5 and Movie S4) and dynamic (Movie S5) pressures better than the existing superhydrophobic and superoleophobic surfaces (*26*). The doubly re-entrant structures allow droplets to bounce on even extremely sparse posts (i.e., tens of micrometers pitch and a solid fraction only ~5%). With high-speed imaging, water, methanol and FC-72 droplets were confirmed to bounce off the truly superomniphobic SiO_2 surfaces (Movie S5). Water (γ = 72.8 mN/m) and methanol (γ = 22.5 mN/m) droplets rebounded on a surface with microposts of 100 μm pitch, which is much larger than those reported in the literature (*3*, *15*). However, FC-72 (γ = 10 mN/m) droplets penetrated and wetted the above surface at impact. A surface with uniformly halved structures (i.e., f_s remaining at ~5%) was further prepared to provide enough resistance against impalement and let FC-72 droplets rebound, as shown with snapshots in Fig. 4C. We note that, while resisting the physical intrusion of liquids, this surface has no defense against some other intrusion mechanisms such as condensation inside the cavity. The internal condensation would be a common issue to all existing superhydrophobic and superoleophobic surfaces (*1*), calling for a provision (*5*) for practical utilization.

Since the proposed super-repellency depends only on physical attributes, we further fabricated metal (i.e., tungsten) and polymer (i.e., parylene) counterparts based on the given SiO_2 surface and confirmed they possess the same super-repellency as expected (fig. S4A). The ability to repel fluorinated solvents may allow the electronic circuits to be cooled by nucleate boiling (i.e., the most efficient mode of cooling) for supercomputers (*4*). Free of polymeric coating, the superomniphobic SiO_2 surface can serve at high temperatures. The surface was found unaltered after a storage at > 1000°C and used to demonstrate rolling-off of another FC liquid at 150°C and a non-volatile liquid at > 320°C (fig. S8 and Movie S6). The polymer-free parts are expected to last longer in outdoor environment, where polymeric materials tend to degrade faster. Unaffected by the surface chemistry, the superomniphobic SiO_2 surface also demonstrated prolonged repellency to biological fluids (sheep serum tested), while a regular superhydrophobic surface lost the repellency (fig. S9 and Movie S7).

References and Notes:

1. D. Quéré, Non-sticking drops. *Rep. Prog. Phys.*. **68**, 2495 (2005).
2. W. Barthlott, C. Neinhuis, Purity of the sacred lotus, or escape from contamination in biological surfaces. *Planta*. **202**, 1–8 (1997).
3. X. Deng, L. Mammen, H.-J. Butt, D. Vollmer, Candle Soot as a Template for a Transparent Robust Superamphiphobic Coating. *Science*. **335**, 67–70 (2012).

4. A. R. Betz, J. Jenkins, C.-J. Kim, D. Attinger, Boiling heat transfer on superhydrophilic, superhydrophobic, and superbiphilic surfaces. *Int. J. Heat Mass Transf.*. **57**, 733–741 (2013).

5. C. Lee, C.-J. Kim, Underwater restoration and retention of gases on superhydrophobic surfaces for drag reduction. *Phys. Rev. Lett.*. **106**, 014502 (2011).

6. T.-S. Wong *et al.*, Bioinspired self-repairing slippery surfaces with pressure-stable omniphobicity. *Nature*. **477**, 443–447 (2011).

7. P. J. Marto, W. M. Rohsenow, Effects of Surface Conditions on Nucleate Pool Boiling of Sodium. *J. Heat Transf.*. **88**, 196–203 (1966).

8. R. L. Webb, The evolution of enhanced surface geometries for nucleate boiling. *Heat Transf. Eng.*. **2**, 46–69 (1981).

9. C.-J. Kim, *Structured Surfaces for Enhanced Nucleate Boiling*. (M.S. Thesis, Iowa State University: 1985).

10. V. P. Carey, *Liquid-vapor phase-change phenomena an introduction to the thermophysics of vaporization and condensation processes in heat transfer equipment* (Hemisphere Pub. Corp., Washington, D.C, 1992).

11. T. Onda, S. Shibuichi, N. Satoh, K. Tsujii, Super-Water-Repellent Fractal Surfaces. *Langmuir*. **12**, 2125–2127 (1996).

12. C.-H. Choi, C.-J. Kim, Large slip of aqueous liquid flow over a nanoengineered superhydrophobic surface. *Phys. Rev. Lett.*. **96**, 066001 (2006).

13. A. Tuteja *et al.*, Designing superoleophobic surfaces. *Science*. **318**, 1618–1622 (2007).

14. A. K. Kota, Y. Li, J. M. Mabry, A. Tuteja, Hierarchically Structured Superoleophobic Surfaces with Ultralow Contact Angle Hysteresis. *Adv. Mater.*. **24**, 5838–5843 (2012).

15. A. Tuteja, W. Choi, J. M. Mabry, G. H. McKinley, R. E. Cohen, Robust omniphobic surfaces. *Proc. Natl. Acad. Sci.*. **105**, 18200–18205 (2008).

16. A. Grigoryev, I. Tokarev, K. G. Kornev, I. Luzinov, S. Minko, Superomniphobic magnetic microtextures with remote wetting control. *J. Am. Chem. Soc.*. **134**, 12916–12919 (2012).

17. R. Dufour *et al.*, Engineering sticky superomniphobic surfaces on transparent and flexible PDMS substrate. *Langmuir*. **26**, 17242–17247 (2010).

18. R. Hensel *et al.*, Tunable nano-replication to explore the omniphobic characteristics of springtail skin. *NPG Asia Mater.*. **5**, e37 (2013).

19. D. Brutin *et al.*, Sessile drop in microgravity: creation, contact angle and interface. *Microgravity Sci. Technol.*. **21**, 67–76 (2009).

20. D. Janssen, R. De Palma, S. Verlaak, P. Heremans, W. Dehaen, Static solvent contact angle measurements, surface free energy and wettability determination of various self-assembled monolayers on silicon dioxide. *Thin Solid Films*. **515**, 1433–1438 (2006).

21. C. Urata, B. Masheder, D. F. Cheng, A. Hozumi, Unusual Dynamic Dewetting Behavior of Smooth Perfluorinated Hybrid Films: Potential Advantages over Conventional Textured and Liquid-Infused Perfluorinated Surfaces. *Langmuir*. **29**, 12472–12482 (2013).

22. L. Feng *et al.*, Petal effect: a superhydrophobic state with high adhesive force. *Langmuir*. **24**, 4114–4119 (2008).

23. A. Cassie, S. Baxter, Wettability of porous surfaces. *Trans. Faraday Soc.*. **40**, 546–551 (1944).

24. T. Liu, C.-J. Kim, in *Proc. Int. Conf. Solid State Sensors, Actuators and Microsystems (Transducers'13)* (2013).

25. Y. Ma, X. Cao, X. Feng, Y. Ma, H. Zou, Fabrication of super-hydrophobic film from PMMA with intrinsic water contact angle below 90°. *Polymer*. **48**, 7455–7460 (2007).

26. R. Hensel *et al.*, Wetting Resistance at Its Topographical Limit: The Benefit of Mushroom and Serif T Structures. *Langmuir*. **29**, 1110–1112 (2013).

27. This general definition of f_s and f_g follows Cassie and Baxter's original paper, which included all the non-flat (e.g., rough, curved) effect on the liquid-solid and liquid-vapor interface. In addition to the most simplified version of flat liquid-solid and flat liquid-vapor interfaces, which results in $f_s + f_g = 1$, often adopted in the literature is a less simplified version of non-flat liquid-solid and flat liquid-vapor interfaces.

28. Materials and methods are available as supplementary material on *Science* Online.

29. Those liquids are commonly used for applications such as electrochemistry, fuel cell, semiconductor industry, microfluidic systems, heat transfer, etc.

30. C. G. L. Furmidge, Studies at phase interfaces. I. The sliding of liquid drops on solid surfaces and a theory for spray retention. *J. Colloid Sci.* **17**, 309–324 (1962).

31. W. Choi, A. Tuteja, J. M. Mabry, R. E. Cohen, G. H. McKinley, A modified Cassie-Baxter relationship to explain contact angle hysteresis and anisotropy on non-wetting textured surfaces. *J. Colloid Interface Sci.* **339**, 208–216 (2009).

32. M. Reyssat, D. Quéré, Contact Angle Hysteresis Generated by Strong Dilute Defects. *J. Phys. Chem. B*. **113**, 3906–3909 (2009).

33. R. Raj, R. Enright, Y. Zhu, S. Adera, E. N. Wang, Unified Model for Contact Angle Hysteresis on Heterogeneous and Superhydrophobic Surfaces. *Langmuir*. **28**, 15777–15788 (2012).

34. P. Papadopoulos, L. Mammen, X. Deng, D. Vollmer, H.-J. Butt, How superhydrophobicity breaks down. *Proc. Natl. Acad. Sci.* **110**, 3254–3258 (2013).

35. A. K. Epstein, T.-S. Wong, R. A. Belisle, E. M. Boggs, J. Aizenberg, Liquid-infused structured surfaces with exceptional anti-biofouling performance. *Proc. Natl. Acad. Sci.* **109**, 13182–13187 (2012).

36. S. Lewin, Blood Serum Surface Tension and its Potential. *Br. J. Haematol.* **22**, 561–566 (1972).

Acknowledgments: C.-J. K was encouraged by D. Attinger to start this research. T. L. acknowledges W. Choi and K. Ding on discussion of the fabrication, L.-X. Huang for assistance with high-speed imaging, and K. Shih for help with roll-off angles measurements. Both thank the anonymous referee for advice on biofouling test, D. Di Carlo and O. Adeyiga for biofluid selection, B. Dunn, R. Freeman, and S. Chen for manuscript preparation. The data reported in the paper are tabulated in the Supplementary Materials. A patent has been filed on this work by C.-J. Kim and T. Liu, "Liquid-Repellent Surface Made of Any Materials," International Application No. PCT/US2014/57797.

Supplementary Materials:

Materials and Methods

Supplementary Text

Figs. S1-S9

Tables S1-S2

Movies S1-S7

References (*30-36*)